Biofilm reactor staging influences microbial community composition and diversity of under denitrifying conditions - Implications for pharmaceutical removal

Elena Torresi[1,2,**], Arda Gulay[1], Fabio Polesel[1], Marlene M. Jensen[1], Magnus Christensson[2], Barth F. Smets[1*], Benedek Gy. Plósz[1,3]

[1]DTU Environment, Technical University of Denmark, Bygningstorvet B115, 2800 Kongens Lyngby, Denmark

[2]Veolia Water Technologies AB, AnoxKaldnes, Klosterängsvägen 11A, SE-226 47 Lund, Sweden

[3]Department of Chemical Engineering, University of Bath, Claverton Down, Bath BA2 7AY, UK

[*]Corresponding authors: elto@env.dtu.dk, bfsm@env.dtu.dk

Abstract

The subdivision of biofilm reactor in two or more stages (i.e., reactor staging) could represent an option for process optimisation of biological treatment. The biofilm exposure to different influent organic carbon (induced by the staging) can influence microbial activity and, above all, diversity, likely resulting in positive implications on removal of micropollutants. In this study, we investigated the microbial composition and diversity of denitrifying Moving Bed Biofilm Reactors (MBBRs) operated under a three- (S) and single-stage (U) system configuration, while also evaluating denitrification and removal of pharmaceuticals. The effect of long-term exposure (471 days) on microbial community to varying organic carbon type and loading of influent wastewater was assessed through (i) 16S rRNA amplicon libraries and (ii) quantitative PCR (qPCR) targeting relevant denitrifying genes. Significantly higher microbial richness was measured in the staged MBBR (at 99% sequence similarity) compared to single-stage MBBR. A more even and diverse microbial community was selected in the last stage of S (S3), likely due to carbon limitation exposure during continuous-flow operation. Additionally, MBBR staging selected for specific taxa (i.e., *Candidate division WS6* and *Deinococcales*) and higher abundance of *atypical nosZ* in S3. While the staged system consistently achieved higher denitrification rates (up to 30%) during continuous-flow operation, no major differences between staged- and single-stage configurations were observed in terms of removal efficiency or rate constants of targeted pharmaceuticals (e.g., sulfamethoxazole, atenolol, citalopram). A positive correlation ($p<0.05$) between removal rate constants of several pharmaceuticals with denitrification rates and abundance of relevant denitrifying genes was observed, but not with biodiversity. Despite the previously suggested positive relationship between microbial diversity and functionality in macrobial and microbial ecosystems, this relationship was not observed in the current study.

Keywords: Moving Bed Biofilm Reactors, micropollutant removal, organic carbon, structure-function relationships; heterotrophic denitrification

1. Introduction

The presence of micropollutants (e.g., pharmaceutical and personal care products) in municipal wastewater effluent is well documented (Barbosa et al., 2016; Dickenson et al., 2011) and has been associated to several environmental risks (Jobling et al., 1998; Painter et al., 2009).

Existing processes in conventional wastewater treatment plants (WWTPs) do not represent a complete barrier for the release of micropollutants with effluent wastewater streams (Carballa et al., 2004). Hence, a number of engineering solutions are being explored to optimize removal of micropollutants via biological wastewater treatment (Falås et al., 2016; Petrie et al., 2014; Torresi et al., 2017, 2016b).

The subdivision of biological reactors in two or more stages (i.e. reactor staging) has recently been proposed to enhance the removal of conventional pollutants (i.e., organic carbon, nitrogen) and pharmaceuticals in biofilm systems such as Moving Bed Biofilm Reactors (MBBRs) (Escolà Casas et al., 2015; Polesel et al., 2017). In MBBRs, biofilms grow on specifically designed plastic carriers, which are suspended and retained in the system (Ødegaard, 1999).

Due to presence of different fractions of organic carbon (e.g., from readily to slowly biodegradable) in wastewater (Roeleveld and Van Loosdrecht, 2002), biofilm in staged MBBR systems can be exposed to different substrate availability conditions in the different stages, potentially leading to different microbial activities in each stage (Polesel et al., 2017). Based on long and short-term laboratory experiments, our previous work showed that the first stage of ustaged MBBR system is effectively exposed to higher loadings of easily degradable organic carbon compared to the last stage, leading to a decrease of denitrification and pharmaceutical biotransformation rate constants in the three sub-stages (Polesel et al., 2017). However, it is unclear whether the gradient of degradable organic carbon, induced by the staging, influenced the microbial community structure and diversity of the biofilm in the multi-stage MBBR

system in comparison to a single stage configuration. Gradients in concentration and composition of dissolved organic carbon have previously been shown to differently shape the structure and diversity of field- (Li et al., 2014) and laboratory-scale (Li et al., 2012) aquifer sediment microbial communities, and influenced the attenuation of several micropollutants in these systems (Alidina et al., 2014). The microbial communities in sediments receiving more refractory carbon were more diverse and more capable of micropollutant attenuation (Alidina et al., 2014).

Hence, elucidating the microbial structure and diversity of biofilms and its influence on the overall microbial activity is fundamental for providing a basis to improve design and operation of MBBR towards pharmaceuticals removal. Additionally, although denitrification is a widespread process in biological wastewater treatment, substantial knowledge gaps remain concerning microbial communities under denitrifying condition (Lu et al., 2014).

Investigating microbial composition and diversity (i.e., alpha-diversity) in biological systems appears especially important when assessing rare microbial activities, such as biotransformation of micropollutants (Helbling et al., 2015; Johnson et al., 2015a). The existence of a relationship between microbial diversity and activity has been debated but a positive relationship between biodiversity and ecosystem functionality is commonly accepted (Briones and Raskin, 2003; Cardinale, 2011; Cardinale et al., 2012). This relationship has been observed with respect to the removal of several micropollutants in both full-scale (Johnson et al., 2015a) and laboratory- bioreactors (Torresi et al., 2016a; Stadler at al., 2016), showing that communities with higher diversity are likely to have more functional traits (Johnson et al., 2015b). Accordingly, biofilms, potentially exhibiting higher microbial niches and thus biodiversity than conventional activated sludge (Stewart and Franklin, 2008), can represent a valid option to enhance micropollutant removal. Furthermore, the exposure of the biofilm to varying carbon types and conditions through bioreactor staging could additionally positively impact their microbial diversity.

In this study we evaluated the long-term effects of three-stage ($S=S_1+S_2+S_3$) and single-stage configurations (U) of pre-denitrifying MBBR on the biofilm microbial community structure and diversity. High-throughput sequencing of 16S rRNA gene amplicon and quantitative PCR (qPCR) was used to asses microbial alpha-diversity at local (S1, S2, S3) and system (S, U) level and the abundance of relevant denitrifying genes, respectively. Thus, the main objectives of the study were:

1) to investigate the effect of organic carbon availability tiered by staging MBBRs on microbial structure and diversity at local and system level, benchmarked to a single-stage configuration;
2) to assess the dynamics in microbial community composition and denitrifying genes abundance in the two MBBR systems during long term operation;
3) to assess associations between micropollutant biotransformation, local/system diversity and denitrifying functionalities.

2. Methods

2. 1. Continuous-flow operation of the MBBRs and batch experiments.

A detailed description of the three- and single stage MBBR systems is reported in Polesel et al. 2017. Briefly, two laboratory scale pre-denitrifying MBBR with K1 carriers (AnoxKaldnes, Lund, Sweden) were operated in parallel under continuous-flow conditions for more than 471 days.

The single-stage system included a single bioreactor (U) with an operating volume of 6 L. The three-stage configuration included three reactors in series (named S1, S2, S3) with a total operating volume of 6 L (1.5 L for S1 and S2 and 3 L for S3). The two configurations were operated under identical conditions (Table S1 in Supplementary Information), i.e. influent flow rate, hydraulic residence time (HRT= 8.9 h), filling ration (33%), ambient temperature, medium characteristics (pre-clarified wastewater from Mølleåværket WWTP, Lundtofte, Denmark), influent nitrate concentration (~103 mgN L^{-1}), sparging of N_2 gas for mechanical mixing and to ensure anoxic conditions in the two systems. The systems were started with MBBR carriers collected from the post-denitrification zone of Sjölunda WWTP (Malmö, Sweden), which had received long-term methanol dosing.

Two batches experiments were performed to assess denitrification rates and biotransformation rate constants of micropollutants at day 100 (Batch 1) and day 471 (Batch 2) of operation. For the batch experiments, the flow to and between reactors was stopped and the reactors were drained. Subsequently, the reactors were filled with pre-clarified wastewater (daily sampled) and carriers from U, S1, S2 and S3 (20% and 10% of filling ratio for Batch 1 and 2, respectively). The experiment lasted for 24 and 49 h for Batch 1 and 2, respectively.

117 **2.2 DNA extraction and quantitative PCR.**

118 To characterize microbial structure and its variation over long term operation of the two MBBR systems,
119 biofilm carriers for each MBBR were collected at day 0 (inoculum sample), 42, 59, 74, 88, 218, 300, 434
120 and 471 of operation. The highest number of samples was taken during the first 100 days of operation,
121 when the biomass was adapting to the new operational conditions (i.e., staged pre-denitrification without
122 methanol addition). Each time, biomass was detached from one carrier using a sterile brush (Gynobrush,
123 Dutscher Scientific) and sterile-filtered tap water, the sample was centrifuged (10000 rpm for 5 minutes),
124 and the supernatant was removed. The sample was stored in sterilized Eppendorf tubes at -20 ^{o}C until
125 further analysis. DNA was extracted from biomass of one carrier using a Fast DNA spin kit for soils (MP
126 Biomedicals, USA) following manufacturer's instructions. The quantity and quality of extracted biofilm
127 DNA were measured and checked by its 260/280 ratio by NanoDrop (Thermo Scientific™). Quantitative
128 PCR (qPCR) was performed to estimate the abundance of total bacteria (EUB) with non-specific 16S
129 rRNA gene targeted primers, and the abundance of a suite of genes encoding relevant functions: nitrate
130 reductase (*narG*), cytochrome cd1 and copper nitrite reductases, *nirK* and *nirS,* respectively (Philippot
131 and Hallin, 2005), nitrous oxide reductase of the *Proteobacteria nosZ* variant (*nosZ* typical) and of the
132 *Bacteroidetes nosZ* variant (*nosZ* atypical). Reported total microbial abundances are expressed as number
133 of gene copies per gram of biomass, while ratios were calculated on the absolute copies number per
134 ngDNA. Primers and conditions for quantification of each gene are listed in Table S2.

135

136 **2.3. 16S rRNA gene amplification, sequencing and bioinformatic analysis.**

137 PCR amplification and sequencing were performed at the DTU Multi Assay Core Center (Kgs Lyngby,
138 DK). Briefly, DNA was PCR amplified using 16S rRNA bacterial gene primers PRK341F (5'-
139 CCTAYGGGRBGCASCAG-3') and PRK806R (5'-GGACTACNNGGGTATCTAAT-3')(Yu et al.,

2005) targeting the V3 and V4 region. PCR products were purified using AMPure XP beads (Beckman-Coulter) prior to index PCR (Nextera XT, Illumina) and sequencing by Illumina MiSeq. Paired-end reads were assembled and screening was implemented using mothur (Schloss, 2009). High quality sequences were then transferred to the QIIME environment and OTUs were picked at 93, 95, 97 and 99% sequence similarity using the UCLUST algorithm (Edgar et al., 2011) with default settings, and representative sequences from each were aligned against the Silva123_SSURef reference alignment using SINA algorithm (Quast et al., 2013). Aligned sequences were then used to build phylogenetic trees using the Fast Tree method (Price et al., 2009).

Taxonomy assignment of each representative sequence at all similarity levels was implemented using the BLAST algorithm (Altschul et al., 1997) against the Silva128_SSURef database. Sequences with reference sequence hit below 90% were called unclassified. Subsampling at depth of 14.000 sequences was performed to equalize sample sizes for further analysis.

Meta communities were created by combining OTU libraries of S1, S2 and S3 reactors and adding into the OTU tables of original samples for further subsampling process. Alpha diversity of OTU libraries was measured using the Chao1, Shannon, and ACE metrics as implemented in R using Phyloseq package (McMurdie and Holmes, 2013). Microbial evenness was estimated as H1/H0 as described in Johnson et al. (2015a). Distance matrices were constructed using the Bray-Curtis (Bray and Curtis, 1957) algorithms in R. Moving windows analysis were implemented using the microbial community of the inoculum as the reference point as described in Marzorati et al. (2008). Most abundant taxa and enriched taxa in S and U reactors were visualized using the Pheatmap package in R. Top 50 taxa were selected and compared within the samples taken after 200 days of operation.

2.4 Denitrification in continuous-flow and batch experiments

During continuous-flow operation, system denitrification performance in the two MBBR systems was assessed by measuring (i) COD removal rate r_{COD} (gCOD m^{-2} d^{-1}) normalized per available surface area (Table S1) per reactors calculated from influent and effluent COD concentration at each stage; (ii) denitrification rate normalized per surface area of reactor $r_{NOx\text{-}N}$ (gN m^{-2} d^{-1}) calculated from influent and effluent concentration of NO_X-N (accounting for both NO_3-N and NO_2-N; Sözen et al., 1998) at each stage. Measurements were taken biweekly during the first 100 days operation to ensure stable start-up of the systems and bi-monthly subsequently.

During batch experiments, biomass specific denitrification rates $\bar{k}_{NOX}$ (mgN g^{-1} d^{-1}) were derived through linear regression of NO_X-N utilization curves for each sub-stage MBBR (Polesel et al., 2017). Specific denitrification rate at system level in S was calculated according to Eq. 1:

$$k_{NOX,S} = \frac{k_{NOX,S1} * X_{S1} * V_{S1} + k_{NOX,S2} * X_{S2} * V_{S2} + k_{NOX,S3} * X_{S3} * V_{S3}}{\sum X_{SMBBR} * V_S} \quad \text{(Eq.1)}$$

Where $\bar{k}_{NOX,S1}$, $\bar{k}_{NOX,S2}$, $\bar{k}_{NOX,S3}$ indicate specific denitrification rates in S1, S2 S3 respectively, X (g L^{-1}) and V (L) at the nominator the biomass concentration (expressed in g of Total Suspended Solids, TSS) and the volume of each MBBR stage, and X_{SMBBR} (g L^{-1}) and V_S (L) at the denominator, the biomass and volume of the staged system as a total MBBR (S).

2.5 Micropollutants in continuous-flow and batch experiments

Only indigenous pharmaceuticals occurring in municipal wastewater were quantified, as no reference pharmaceuticals were spiked during continuous-flow and batch experiments. Twenty-three pharmaceutical, typically present in wastewater influents (Margot et al., 2015), were targeted which

includes six groups of compounds: beta-blocker, sulfonamide antibiotics sulfadiazine, anti-inflammatory, antiepileptic/ antidepressants pharmaceuticals, X-ray contrast media. The complete list of targeted pharmaceuticals is reported in section S1 of the Supplementary Information.

Continuous-flow samples were taken in two separate sampling campaigns (lasting 5 and 3 days, respectively), before the execution of Batch 1 (100 days) and 2 (471 days) experiments. Removal efficiencies were calculated by measuring influent and effluent concentration in the two systems (Polesel et al., 2017).

During batch experiments three main micropollutant removal mechanisms were observed: (1) biotransformation, (2) retransformation to parent compounds (i.e., deconjugation), (3) enantioselective biotransformation (Polesel at el., 2017). Pseudo first-order transformation kinetics k_{Bio} (1, L g^{-1} d^{-1}), retransformation rates k_{Dec} (2, L g^{-1} d^{-1}), biotransformation rate constant of enantiomer 1 and 2, $k_{bio,1}$ and $k_{bio,2}$, (3, L g^{-1} d^{-1}) were estimated as described in Polesel et al., 2017 using the Activated Sludge Model framework for Xenobiotics (ASM-X) (Plósz et al., 2012).

Subsequently, the estimated k_{Bio} and k_{Dec} in each sub-reactor of the staged MBBR configuration (Table S3) were used to calculate (i) system-level biotransformation /retransformation rate for S for each micropollutant and (ii) collective rate constants of multiple pharmaceuticals.

(i) As described for specific denitrification rate (Eq. 1), system-level $k_{Bio,S}$ (and similarly $k_{Dec,S}$) were calculated according to Eq. 2:

$$k_{\mathrm{Bio,S}} = \frac{k_{\mathrm{Bio,S1}} * X_{S1} * V_{S1} + k_{\mathrm{Bio,S2}} * X_{S2} * V_{S2} + k_{\mathrm{Bio,S3}} * X_{S3} * V_{S3}}{\sum X_{SMBBR} * V_S} \quad \text{(Eq.2)}$$

(ii) Additionally, to compare the performance of each sub-stage of S MBBR with U MBBR in terms of micropollutant biotransformation, we assessed the collective rate constants of

multiple pharmaceuticals biotransformation and retransformation (*collective* k_{BioS1}/k_{DecS1}, k_{BioS2}/k_{DecS2}, k_{BioS3}/k_{DecS3}, k_{BioU}/k_{DecU}). The rates were calculated by scaling each compound's normalized rate (mean of 0, standard deviation of 1) and averaging of the scaled rates, as previously considered (Johnson et al., 2015a; Zavaleta et al., 2010).

2.6 Analytical methods

All the samples taken for analysis of conventional pollutants i.e., NO_3-N, NO_2-N, NH_4-N, soluble COD (sCOD) and biomass concentration in both continuous operation and batch experiments were previously described in Polesel et al., 2017. Wastewater fractionation to assess, e.g., biodegradable COD and the two fractions, readily biodegradable COD and slowly biodegradable COD was performed according to Roeleveld and Van Loosdrecht (2002).

Samples for micropollutants were frozen at -20 °C prior analysis and analyzed using HPLC-MS/MS as described in Escolà Casas et al. (2015). Information regarding targeted micropollutants, HPLC-MS/MS and mass spectrometry conditions, limit of quantification and detection are shown in Escolà Casas et al. (2015).

2.7 Statistical analysis.

Correlation between k_{Bio}, k_{Dec}, *collective* rate constants k_{Bio}/k_{Dec}, denitrification rates $\bar{k}_{NOX}$ and biodiversity indices (Shannon, ACE, Chao and evenness indices) was assesses using in Graph Prism 5.0. The statistical methods comprise (i) one way analysis of variance (ANOVA) with Bonferroni post-hoc test (significance level at $p<0.05$); (ii) Pearson correlation analysis (r values reported) and adjusted p-values (two-tailed). Although, Wilk-Shapiro test of normality may suggest a normal distribution ($p<0.05$)

229 as the underlying distribution for the obtained biotransformation rate constants, bias could occurred due
230 to the small sample size (equal to 4). Pearson coefficients were reported as an indication of the strength
231 of the association between the targeted parameters and micropollutant biotransformation rate constants.

3. Results and discussion

3.1 Comparison of continuous-flow operation performance in S and U MBBR systems

3.1.1. Denitrification

The loading of readily biodegradable (S_S) and hydrolysable (X_S) fractions of COD in influent wastewater varied significantly through the experimental time (Fig. S1), with X_S typically contributing to more than 50% of biodegradable COD (bCOD). Most of influent S_S was utilized in the first stage S1 (on average 70%, Fig. S2a), leading to lower carbon loadings in the following stages (1.6 ± 0.4, 0.78 ± 0.2, 0.6 ± 0.2 gCOD d^{-1} in S1, S2, S3 respectively, Polesel et al., 2017). A decrease in the surface-normalized COD removal rates (r_{COD}, gCOD d^{-1} m^{-2}) could be observed after approximately 70 days of operation for the staged and un-staged MBBR, respectively, due to differences in carbon loading (Fig. S1). Except for few sampling days where r_{COD} in the staged MBBR was higher (up to 2-fold) than in the un-staged MBBR, no major differences in removal of COD were observed in the two systems (Fig 1a). Higher variability of performance was observed in the removal of nitrogen species NO_X-N (Fig 1b). The three-stage MBBR generally outperformed the single-stage system (higher up to 30%, for ~ 60% measurements) in terms of $r_{NOx\text{-}N}$ after 50 days of operation. Fluctuations in $r_{NOx\text{-}N}$ were also caused by the variance in the influent bCOD. Biomass concentration (as gTSS L^{-1}) rapidly increased in the first 100 days of operation (Fig. S3), reaching values (average ± standard deviation) of 4.9 ± 0.9, 5.2 ± 1.9, 4.7 ± 1.2, 4.47 ± 1.3 g L^{-1}, for S1, S2, S3 and U, respectively.

Overall, data during continuous-flow operation suggest an enhancement in denitrification performance in the three-stage MBBR, possibly explained based on reaction kinetics principles (Plósz, 2007), e.g., maximization of the uptake rate of S_S and less degradable carbon in the stages of S configuration.

Additionally, differences in nitrogen oxide reduction with a similar COD utilization were also observed during batch experiments, resulting in different calculated observable yield $Y_{H,obs}$ (mgCOD mgCOD^{-1}) in the four MBBRs (Polesel et al., 2017).

3.1.2 Micropollutant removal

During continuous-flow operation, 11 of the 23 targeted compounds were detected in the pre-clarified wastewater, including compounds such as atenolol, citalopram, diclofenac, sulfamethoxazole, erythromycin and iohexol (Fig. 1 c, d). Removal efficiencies of micropollutants (calculated according to Eq. S2) during the two sampling campaigns (at ~100 and 470 days of operation) were compound dependent, with atenolol and citalopram having the highest removal (72% and 56–67%, respectively) and sulfamethoxazole a negative removal (> -150%) due to possible de-conjugation of human metabolites (Polesel et al., 2017). The removal efficiency of the measured pharmaceuticals was not significanlyt different between U and S MBBR system in the two sampling campaigns (Fig. 1c,d).

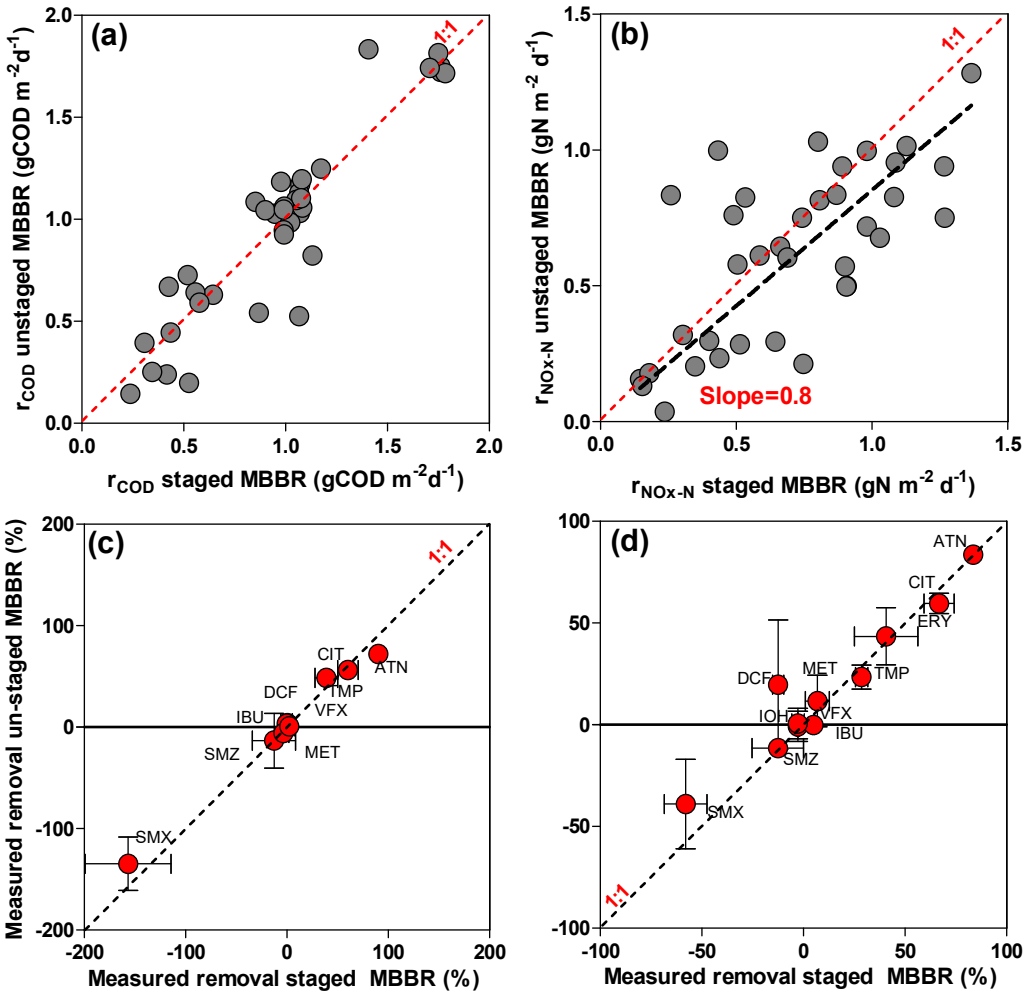

271

272 **Figure 1.** Measured data from continuous-flow operation. Comparison between COD removal rates (r_{COD}, gCOD
273 d^{-1} m^{-2}) and denitrification rate (r_{NOx-N}, gN m^{-2} d^{-1}) in the staged and un-staged MBBR (a and b); comparison
274 between micropollutant removal (%) in S and U in the first (c, ~100 days of operation) and second (d, ~470 days
275 of operation) campaigns. Dashed black line in (b) shows linear regression (slope 0.80 ± 0.07). Abbreviations: ATN
276 = atenolol; CIT = citalopram; TMP = trimethoprim; DCF = diclofenac; IBU= ibuprofen; MET = metoprolol; SMX
277 = sulfamethoxazole; SMZ = sulfamethizole; VFX = venlafaxine; ERY = erythromycin; IOH = iohexol.

278 **3.2 Microbial community structure and diversity in S and U MBBR systems**

279

280 ***3.2.1 Microbial diversity at local and system level***

281 Microbial diversity in the two MBBR systems was assessed at 93%, 95%, 97% and 99% sequencing
282 similarities cut-offs to maximize the resolution of the α-diversity analysis between the four reactors.
283 After implementation of quality control measures, a total of 3178345 high quality sequences were
284 obtained for each clustering, subsequently rarefied to 15800 sequences per sample.

285 Alpha-diversity (expressed as Shannon diversity, ACE and Chao richness indices) increased overall with
286 increasing sequence similarity cut-offs (Fig. 2)– as expected (Birtel et al., 2015). As the two MBBR
287 systems followed similar patterns over the time in terms of community diversity (Fig. 2), the α-diversity
288 was likely influenced by variations in influent wastewater composition (in terms of COD and microbial
289 community in the influent wastewater). Accordingly, linear regression analysis (Fig. S4) suggested a
290 significant ($p<0.05$) positive linear relationship between influent sCOD with microbial richness (ACE
291 and Chao) in U (R^2 of 0.88, n=6) and S1 (R^2 of 0.80, n=6) at 99% similarity, but not for S, S2 and S3.
292 No major differences were observed in terms of Shannon diversity and evenness indices over time
293 between S and U (Fig. 2), while ACE and Chao richness presented overall higher values in S compared
294 to U (with increasing differences at increasing sequences similarity cut-offs, from 23% to 30% for 93%
295 and 99, respectively).

296 Furthermore, we assessed how the difference in the microbial community diversity in S and U (β-
297 diversity) changed over the duration of the experiment and estimated the time needed for the MBBR
298 microbial communities to reach a steady composition that was dissimilar from the inoculum (Fig. 3).
299 Moving window analysis (MWA) was implemented using the reciprocal of Bray-Curtis indices measured
300 at different sequence similarities (Fig. 3). Microbial community similarity significantly decreased from
301 the same inoculum sample during the first 200 days of operation, subsequently reaching a stable

302 composition for the rest of the experiment. Bray-Curtis indices profiles (Fig. 3) for S and U decreased to
303 the highest extent at 99% sequence similarity cut-off.

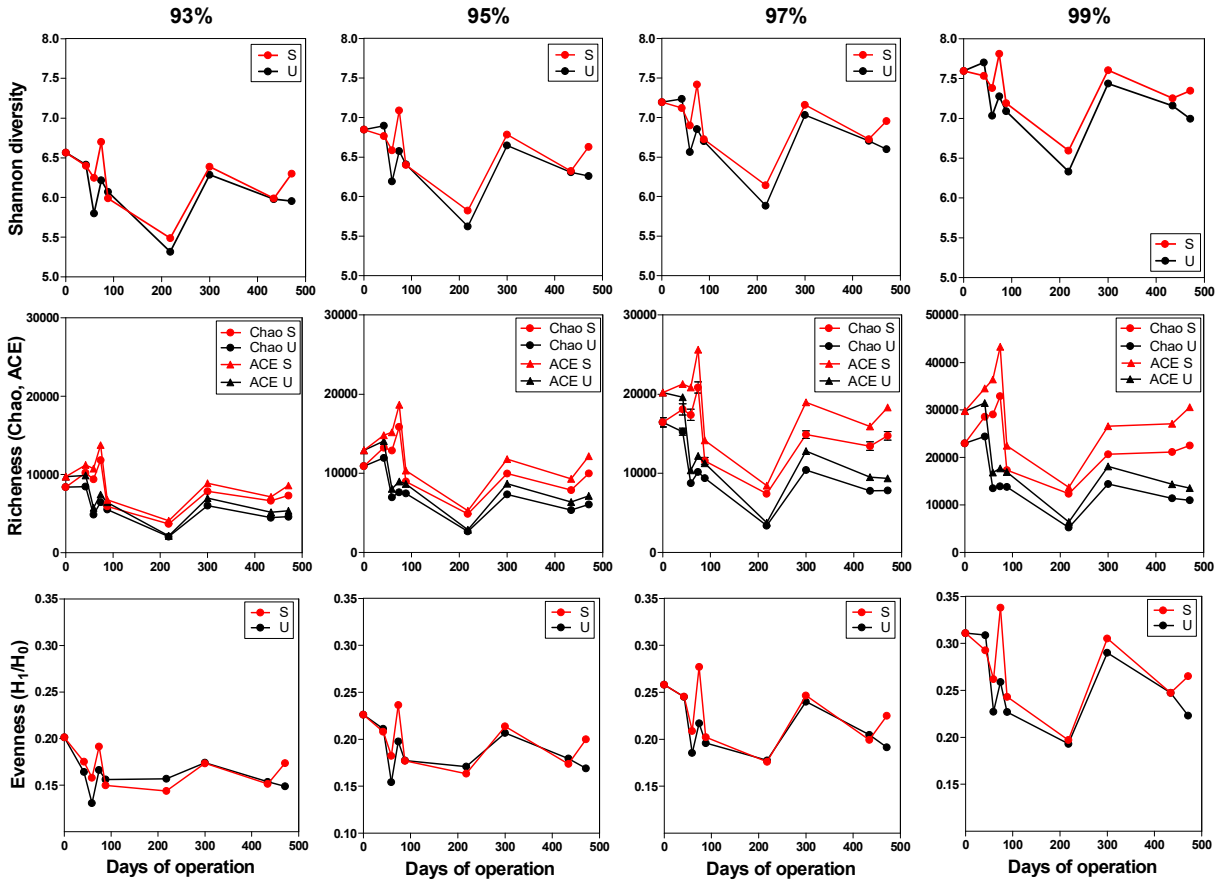

304

305 **Figure 2.** Shannon, richness (Chao and ACE) and evenness (H_1/H_0) indices measured at different time points for
306 the staged (S) and un-staged (U) MBBR at 93, 95, 97 99% of sequencing similarity**.** Error bars define standard
307 errors.

308

309 As the MBBR microbial communities and the difference between them appeared stable after
310 approximately 200 days of operation based on MWA, we averaged the Shannon, richness and evenness
311 indices after 200 days of operation (n=4) to assess statistical difference between the two systems and for

each sub-stage of S (Fig. 4). For all four tested sequence similarity levels, no significant difference was observed for the Shannon diversity and evenness for the microbial communities prevailing in S and U (reported at 97 and 99%, Fig. 4a–b). On the other hand, microbial richness (ACE and Chao) was higher in S than to U at both sequence similarities, with significant difference at 99% sequence similarity cut-off (Fig. 4d).

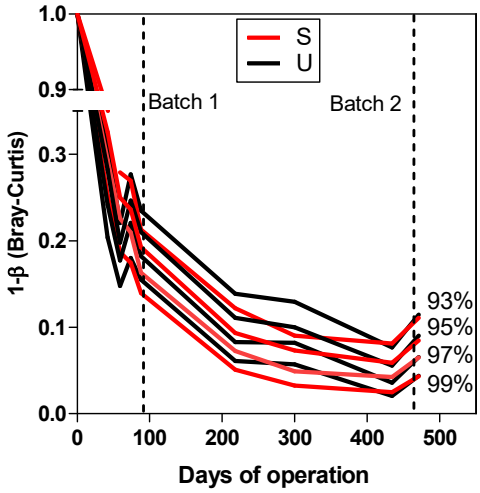

Figure 3. Moving window analysis (MWA) using reciprocal of Bray-Curtis indices (β) from the initial biofilm inoculum measured at different sequence similarity (93-99%) for S and U over 471 days of operation.

Hence, our findings (Fig. 2 and Fig. 4) suggest that the exposure of microbial communities to a gradient of organic carbon, achieved through reactor staging, results in significant higher microbial richness compared to single-stage configuration. Additionally, average Shannon diversity, evenness and richness were higher (although not significantly different) in S3 compared to S1 and S2 at 99% sequence similarity (Fig. 4). Nonetheless, it is likely that the more refractory and slowly biodegradable carbon, to which S3 was exposed during continuous-flow operation (Fig. S2), led to the co-existence of a more

327 diverse microbial community due to substrate competition (Huston, 1994). On the contrary, the easily
328 degradable carbon mostly utilized in S1 may have favoured microbial groups that dominate the microbial
329 community.
330 Similar observations were previously reported in managed aquifer recharge systems (MAR), where
331 higher community diversity was observed at more oligotrophic depths of MAR compared to the depths
332 where more easily degradable carbon was available (Li et al., 2013, 2012). Increased taxonomic richness
333 was also associated with influent lower ambient nitrogen and carbon availability in full-scale wastewater
334 treatment plant microbial communities (Johnson et al., 2015b). Conversely, higher microbial diversity
335 (expressed as Shannon index) was found in the first stage of an aerobic two-stage nitrifying MBBR
336 treating landfill leachate (Ciesielski et al., 2010).

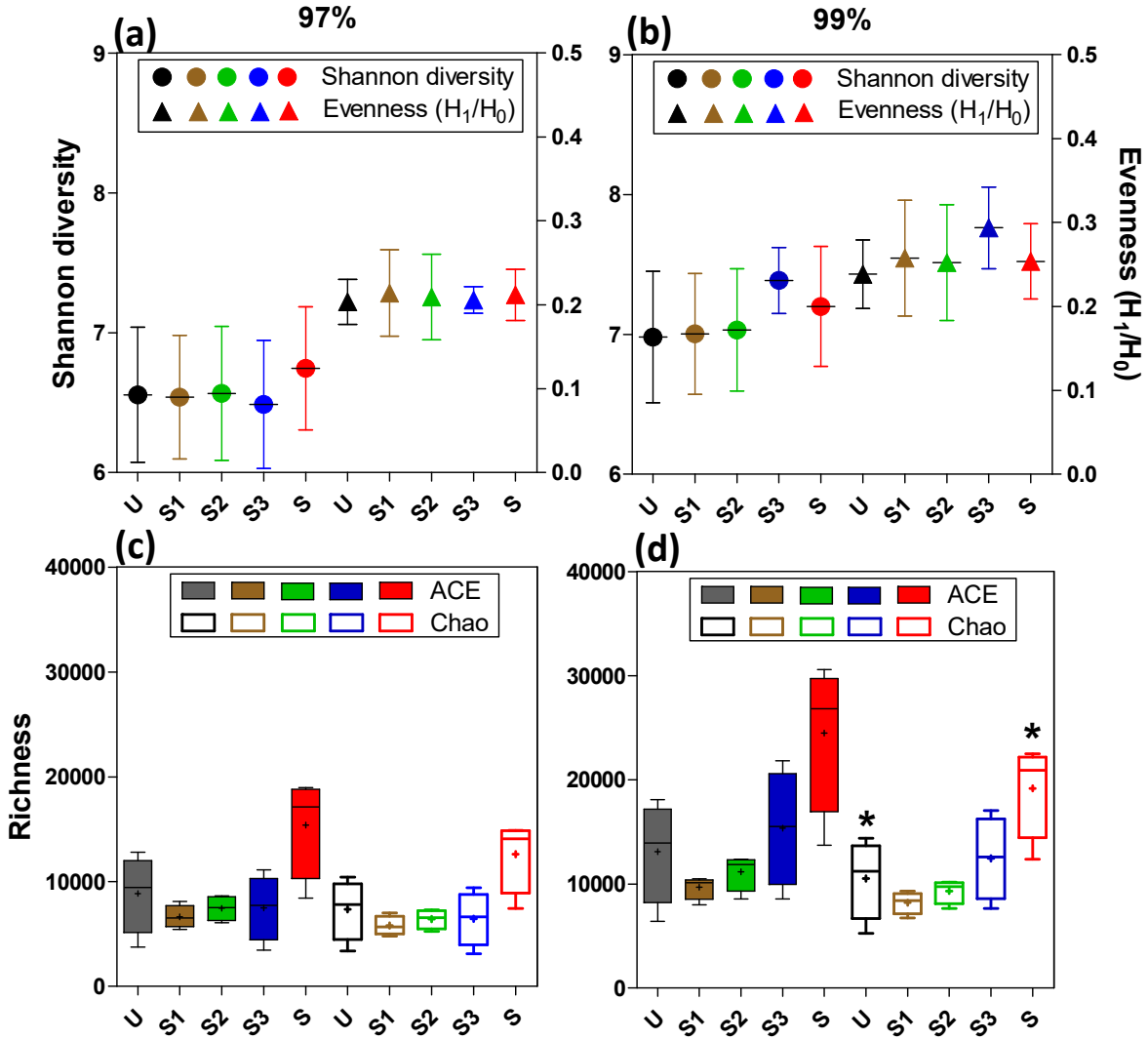

337

338 **Figure 4.** Averaged values of Shannon diversity, evenness, ACE and Chao indices after 200 days of operation
339 (n=4) at 97% (a, c) and 99% (b, d) sequence similarity cut-offs for the three stages MBBR at local (S1, S2, S3)
340 and system (S) level and the single stage system (U). Asterisks indicate significance difference. Mean is shown as
341 +.

342

343

3.2.2 Temporal variability in the selection of taxa by substrate availability in S and U MBRR systems

We further investigated the development of microbial structure in S and U over 471 days of operation to elucidate whether staging the MBBR system resulted in a selection of specific taxa. Hence, we computed heatmaps of the 100 most abundant OTUs at order level sorted by most abundant OTUs after 200 days of operation (218, 300, 434, 471 days) (Fig. 5 (a) and (b)). In both systems, the methanol-utilizing bacteria *Methylophilales*, that were enriched in inoculum (methanol dosing was applied to full-scale WWTP), decreased over time, eventually disappearing after approximately 200 days. A core of OTUs was shared in both systems, consisting of *Burkholderiales*, *Xanthomonadales*, *Flavobacteriales* and *Sphingobacteriales*. Notably, taxa such as *AKYG1722*, *Caldilineales*, *JG30-KF-CM45* and *Candidate division WS6* were enriched in both MBBR systems during 300 days of operation. To effectively identify the microbial organisms that were differently selected in the two configurations, we selected the most abundant OTUs of S and U MBBRs and reported the log of the ratio of the sequence abundance in S and U (log(S/U)) (Fig. 5 (c)). A similar approach was used for the taxa in S3 and S1 ($\log(S_3/S_1)$, Fig. 5 (d)). Notably, staged MBBR (S) selected for the OTU *Bifidobacteriales* and *Candidate division WS6* after day 218. *Candidate division WS6* have been previously identified as abundant community members in anoxic/anaerobic environments (Dojka et al., 1998, 2000). Additionally, *Candidate division WS6* and *Deinococcales* were enriched in S3 over S1 (Fig. 5 (4)), which suggests a correlation of these OTUs with the availability of low readily biodegradable carbon availability at which S3 was operated during continuous-flow operation. The family *Deinococcaceae* is widely studied, since organisms from this groups have been observed to exhibit remarkable resistance to radiation (Chaturvedi and Archana, 2012; Slade and Radman, 2011). Conversely, *Dictyoglomales*, *Microgenomates*_4 and subgroup 4 of *Acidobacteria* were mostly enriched in U over S after 218 days (Fig. 5 (3)). Compared to other subgroups,

367 the abundance of *Acidobacteria subgroup 4* have been negatively associated with organic carbon
368 availability and C-to-N ratio in grassland soils (Naether et al., 2012; Will et al., 2010).
369 Overall, we observed only few taxa consistently enriched after 218 days in the three-stage configuration
370 compared to single-stage and generally dynamic microbial communities. Considering the long-term
371 operation of the two systems with actual pre-clarified wastewater influent, it is likely that, besides the
372 organic substrate availability, continuous and random immigration by the microbial community present
373 in the influent wastewater played an important role in shaping the microbial communities. The
374 importance of microbial immigration was shown by calibrating a neutral model community assembly
375 with dynamic observations of wastewater treatment communities (Ofiteru et al., 2010), in full-scale
376 WWTP (Wells et al., 2014), as well in as a pilot-scale membrane bioreactor system (Arriaga et al., 2016).
377 Additionally, cross-inoculation between staged reactors may have been occurred, as previously observed
378 in staged bioprocesses in full-scale WWTP (Wells et al., 2014).

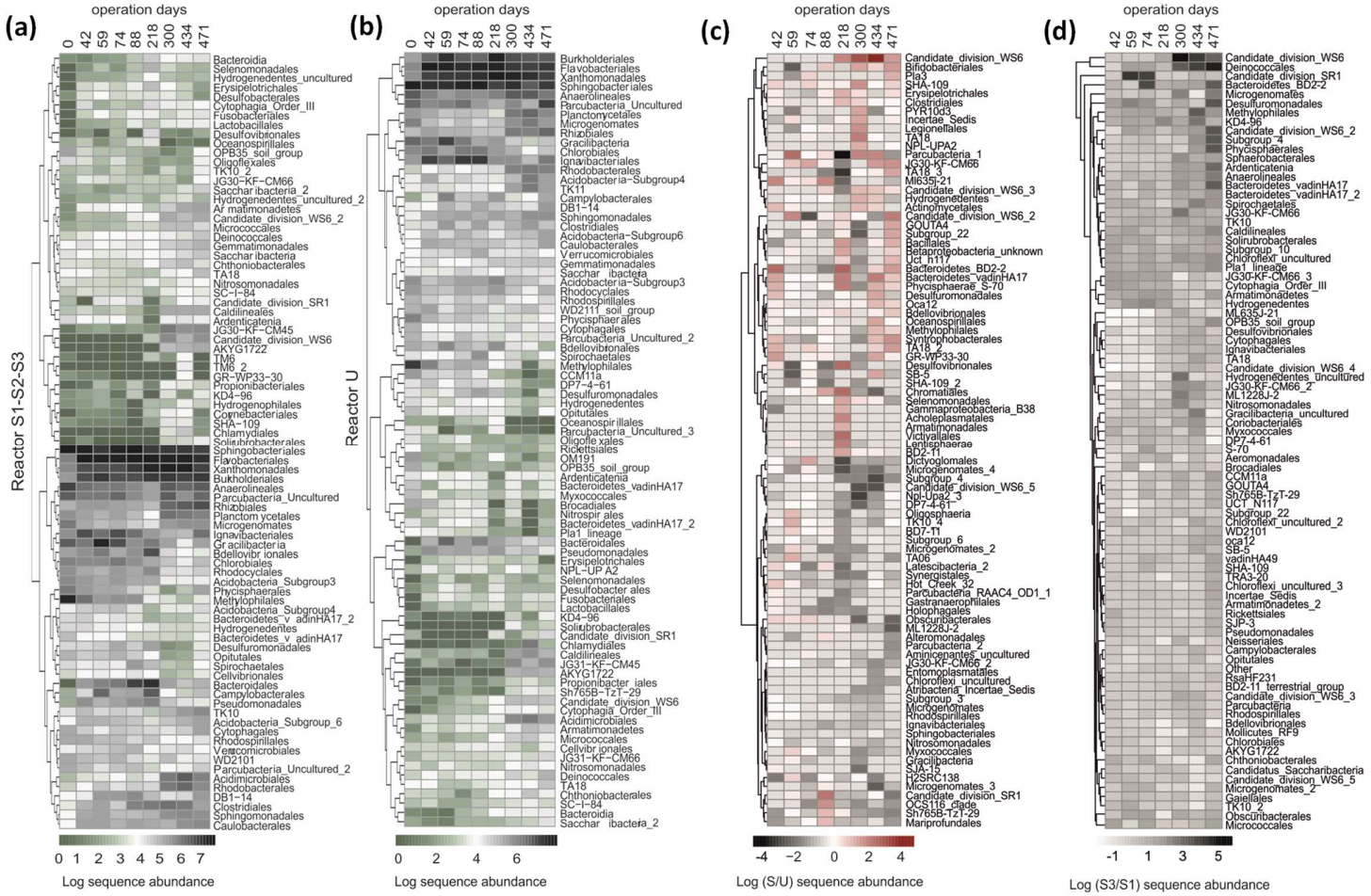

Figure 5. Heatmaps of the 100 most abundant order level taxa in the staged MBBR, S (a) and un-staged MBBR, U (b). The most shifted abundant taxa (expressed as log sequence abundance) of S and S3 were selected to perform the ratio of S/U (c) and S1/S3 (d) to effectively identify the selected taxa in S compared to U, and S3 compared to S1.

3.2.3 Microbial and denitrifying gene abundance in S and U MBBR systems

Quantification of 16S rRNA (total bacteria) and denitrifying genes was performed to investigate differences in denitrifying microbial communities in the four MBBR reactors (Fig. S5). For U and S1 MBBR, microbial abundance of total bacteria during 471 days of operation could be associated with the influent substrate concentration – expressed as influent sCOD (Fig. S6, R^2 of 0.8 and 0.5, respectively), while no association was found for S2 and S3 with the respective influent sCOD.

As informed by MWA, qPCR data for all reactors were averaged from the point when the microbial community was stable (i.e., after 200 days of operation) (Table 1). The lowest abundance of 16S rRNA gene (copies $g_{biomass}^{-1}$) ($p<0.05$) was measured in S3, mostly adapted to carbon limitation during continuous-flow operation, as previously observed in soil-column, simulating managed aquifer recharge (Li et al., 2013). Overall, the measured *nirS* gene fraction was up to 10 times higher than *nirK* (in agreement with other studies in aquatic ecosystems, e.g., Braker et al., 2000; Nogales et al., 2002; Peterson et al., 2011), while no differences was observed between the 4 reactors in terms of *nirS* gene fraction (Table 1). Previous studies have suggested lower densities of *nirK*-containing denitrifiers in aquatic ecosystems (Braker et al., 2000). The decrease of *nirS* from the inoculum sample (day 0), adapted to methanol (Fig. S5), is consistent with the previous observation that utilization of methanol as a readily biodegradable substrate can select for *nirS*-expressing denitrifiers. Furthermore, a change to different carbon sources can result in a loss of *nirS* density (Hallin et al., 2006). The S3 reactor was continuously exposed to the lowest C-to-N influent ratio (average values of C, expressed as soluble COD, -to-N ratio of 1, 0.8 and 0.7 for S1 and U, S2, S3 respectively), and previous research reported increased N_2O production at lower C-to-N ratios (Kampschreur et al., 2009; Zhang et al., 2016). However, S3 (exposed to lower C-to-N ratios during continuous-flow operation) exhibited the highest ($p<0.05$) abundance of atypical *nosZ* gene (% of 16S rRNA, Table 1), which could indicate a more effective N_2O removal with

respect to other reactor stages. Furthermore, S3 and S1 had the highest and lowest ratio of atypical to typical *nosZ*, respectively (Table 1). The typical *nosZ* genes have been associated with bacteria capable of complete denitrification (thus encoding all the enzymes for converting nitrate to nitrogen) (Sanford et al., 2012). In contrast, atypical *nosZ* genes are also found in non-denitrifying bacteria with more-diverse N-metabolism (e.g., missing *nirK* and *nirS*) (Orellana et al., 2014; Sanford et al., 2012), and are commonly present at concentrations higher than typical *nosZ* in soil (Orellana et al., 2014). Hence, our results suggest a microbial selection driven by the substrate gradient through the MBBR stages, where most of the complete denitrifiers (carrying typical *nosZ*) are selected in S1 (with the highest readily biodegradable substrate availability). On the other hand, microbes with more diverse N-metabolism (carrying atypical *nosZ*) are selected in S3. Although, based on prior reports, the highest N_2O production was expected in MBBR stages with low influent C-to-N ratio, the selection of non- denitrifying bacteria containing atypical *nosZ* genes (which code for high affinity N_2O reductase) could have likely reduced the accumulation of nitrous oxide – a factor suggesting staged MBBR as a process optimisation means to reduce N_2O emissions, and which requires further research.

Table 1. Results from qPCR targeting 16S rRNA and functional genes in the four MBBRs (S1, S2, S3, U). Values result from the average of the last four sampling day (218, 300, 434 and 471) after microbial community

47 stabilization according to MWA. Values are reported with the corresponding standard deviation (n=8). Statistical
48 differences ($p<0.05$) were estimated according to one way analysis (ANOVA).

	S1	**S2**	**S3**	**U**
16S rRNA (copies/$g_{biomass}$)	$2.13 \times 10^{11} \pm 44\%$	$1.57 \times 10^{11} \pm 16\%$	$7.24 \times 10^{10} \pm 7\%$ (1)	$2.2 \times 10^{11} \pm 19\%$
narG (%)*	48 ±20	22 ± 7 (2)	53 ±22	27 ± 9
nirS (%)*	58 ± 10	54 ± 9	63 ± 6	64 ± 9
nirK (%)*	8 ± 4	12 ± 7	11 ± 5	11 ± 7
nirS/nirK	6.9 ± 3	8.3 ± 3	6.3 ± 3	10.9 ± 11
nosZ_typ (%)*	9 ± 3	9 ± 1	9 ± 1	9 ± 2
nosZ_atyp (%)*	6 ± 1	8 ± 5	15± 8 (3)	11 ± 5
nosZ_atyp/nosZ_typ	0.72 ± 0.23	0.93 ± 0.53	1.60 ± 0.71 (3)	1.36 ± 0.62

49 * % of 16S rRNA gene abundance

50 (1) significantly lower than S1 and U (95% confidence interval)

51 (2) significantly lower than S1 and S3 (95% confidence interval)

52 (3) significantly higher than S1 and S2 (95% confidence interval)

53

3.3. Linking activity, community structure and diversity with micropollutant biotransformation in batch experiments

3.3.2 System level (S and U)

Based on the results of the batch experiments, biotransformation rate constants of the pharmaceuticals were calculated at system level for the staged MBBR (Eq. 2) and compared with rate constants for the single-stage U MBBR for Batch 1 (Fig. S10) and Batch 2 (Fig. 6 a). We observed an improvement in specific denitrification rate at system level (calculated as in Eq. 1) and higher ($p<0.05$) microbial richenss in S compared to U in Batch 2 (Fig. 6b). Nonetheless, no significant difference was observed in the biotransformation of the targeted micropollutants between the two MBBR systems (Fig S10 and Fig. 6).

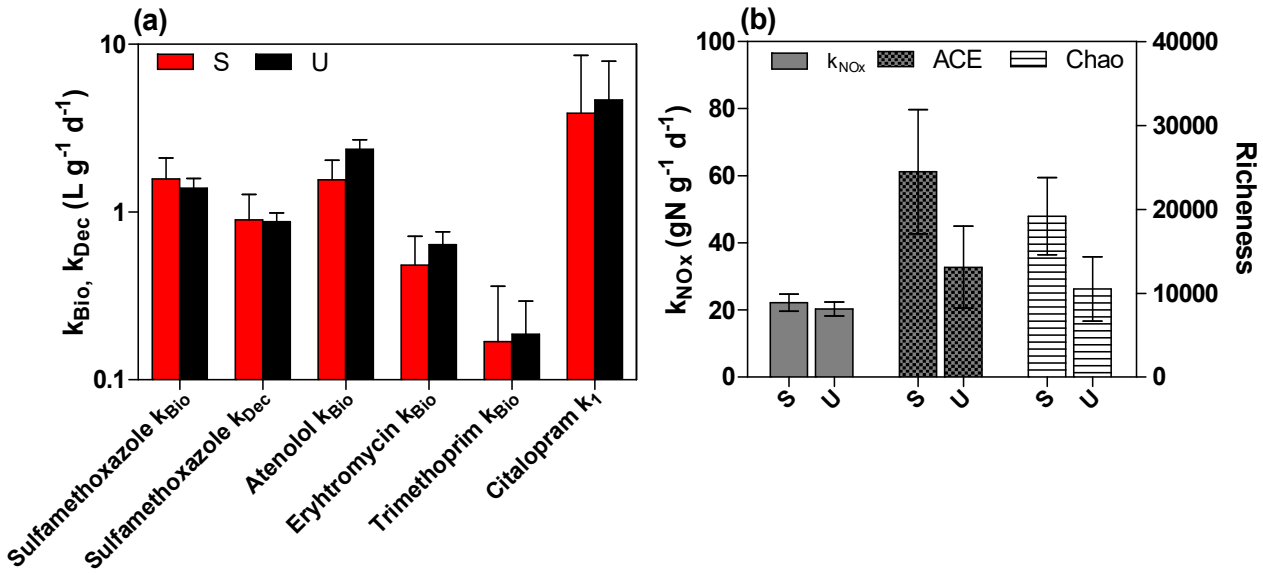

Figure 6. Biotransformation and retransformation rate constants k_{Bio}/ k_{Dec} (L g^{-1} d^{-1}) for each micropollutant (a) and specific denitrification rate, ACE and Chao indices (b) calculated at system level for S for U MBBR in Batch 2.

3.3.1. Local level (S1, S2, S3 and U)

In Batch 1, S1 and U exhibited the highest biotransformation rate constants k_{Bio} (L g^{-1} d^{-1}) for the pharmaceuticals sulfamethoxazole, sulfadiazine, metoprolol, atenolol, up to 4 and 3-fold higher compared to S3, respectively. In Batch 2 (after 471 days of operation) decreased biotransformation kinetics were observed in U, resulting in the highest k_{Bio} obtained for S1 stage reactor for most of the targeted pharmaceuticals (with exception of atenolol) (Polesel et al., 2017). Furthermore, when considering the staged MBBR, k_{Bio} decreased from S1 to S3, consistent with decreasing loading and availability of carbon during continuous-flow operation (Table S3, Polesel et al., 2017).

Pearson's coefficients r were used to evaluate associations between biotransformation rate constant k_{Bio} /k_{Dec} and (i) biodiversity indices (at 99% sequence similarity, Fig. S8); (ii) denitrifying gene abundance (Fig. S5); (iii) specific denitrification rates $\bar{k}_{NOX}$ (mgN g^{-1} d^{-1}) (Table S3). Only relevant k_{Bio} and k_{Dec} values (>0.1 L g^{-1} d^{-1}, according to the classification presented in Joss et al., 2006) were included in the analysis. Notably, in this study correlations were performed by using only taxonomic diversity (based on 16S rRNA amplicon sequencing), rather than data combining functional diversity (based on the phenotypes inferred from taxonomic descriptors and on mRNA sequencing). Although it has been observed that taxonomic and functional diversity associate with each other in wastewater treatment systems (Johnson et al., 2015b), additional information could be derived by the combination of both analysis (Johnson et al., 2015c).

In Batch 1, only few positive correlation ($p<0.05$) were observed between diversity indices and biotransformation rate constants of pharmaceuticals. i.e., sulfamethoxazole, trimethoprim and metoprolol. In Batch 2, k_{Bio} and k_{Dec} of most detected pharmaceuticals were negative or not significant

89 correlated with microbial richness (Fig. 7), but positive correlated ($p<0.05$) with specific denitrification
90 rates k_{NOx}. The obtained correlation are reported in Fig. S7.
91 Positive correlations ($p<0.05$) were also found between k_{Bio} (of erythromycin, trimethoprim and
92 *collective* pharmaceuticals) and the abundance of denitrifying genes *narG*, *nirS*, and *nosZ* typical, but
93 not atypical *nosZ*. The difference in the correlation results from Batch 1 and 2 may derive from adaptation
94 of the biomass to the specific operational conditions (i.e., from post- to pre-denitrification and from single
95 to three-stages configuration). On the other hand, as discussed previously, a stable microbial community
96 was observed only after 200 days of operation and results from Batch 2 (at 471 days) may be considered
97 representative of the long-time operation of the two MBBR systems.
98 Biotransformation of several micropollutants has been related to the lack of specificity (i.e.,
99 cometabolism, Criddle 1993) of enzymes such as ammonia monooxygenase (Sathyamoorthy et al.
100 (2013)). To our knowledge, cometabolism of micropollutants by respiratory denitrifying enzymes (e.g.,
101 *narG*, *nirS*, *nor*, *nosZ*) has not been documented. Thus, the unexpected association between denitrifying
102 genes and biotransformation of micropollutants may be the result of a genuine but nevertheless non-
103 causal relationship (Johnson et al., 2015c). Further research required to examine the cause of this
104 correlation.
105 As mentioned previously, positive relationships between microbial diversity (and in particular α-
106 diversity) and biotransformation rate constants of micropollutants have been observed in activated sludge
107 (Johnson et al., 2015a), in sequencing batch lab-reactors (Stadler and Love, 2016) and in nitrifying
108 MBBRs (Torresi et al., 2016). Yet, equally negatively correlations have been observed between
109 biodiversity and removal of natural and synthetic estrogens in suspended biomass (Pholchan et al., 2013)
110 and of sulfonamides antibiotic (sulfadiazine, sulfamethoxazole, sulfamethizole) in nitrifying MBBRs

111 (Torresi et al., 2016). Among others, two phenomena may explain the lack of an observable (positive)
112 relationship:

113 (i) A positive relationship between biodiversity (or richness) would emerge (a) if the microbial
114 community consisted of a number of microorganisms withe unique niche partioning or (b) if
115 facilitative interactions (i.e., complementarity effects) occurred (Cardinale, 2011; Cardinale
116 et al., 2012; Loreau et al., 2001). However, functional redundancy (i.e., different taxa coexist
117 to perform the same functionality) could be sufficient mask this positive interaction (Johnson
118 et al., 2015b). Accordingly, if the biotransformation of a specific compound is performed by
119 a large number of taxa, the increase of biodiversity may not necessary positively impact the
120 biotransformation as it is not limited by the number of taxa which can perform it (Stadler and
121 Love, 2016). Taken together, the negative correlation observed in this study between
122 biotransformation rate constants and biodiversity, combined with the positive correlation with
123 kinetics of denitrification, could suggest a redundancy of the denitrifying microbial
124 community towards the biotransformation of these targeted pharmaceuticals.
125 This observation might suggest that denitrifying systems exhibit higher biotransformation
126 rates of pharmaceuticals compared to aerobic systems, due to the higher number of taxa
127 performing this function. Hence, we compared the averaged biotransformation rate constants
128 obtained in this study (under pre-denitrification conditions) and in post-denitrification
129 MBBRs (Torresi et al., 2017) with kinetics obtained for aerobic nitrifying MBBRs (Torresi
130 et al., 2016) (Fig S11). While we observed comparable biotransformation kinetics for aerobic
131 and pre-denitrifying MBBRs (this study) (Fig. S11a), post-denitrifying MBBRs indeed
132 exhibited higher biotransformation rate constants for more than 60% of the examined
133 pharmaceuticals (Fig. S11b) compared to aerobic MBBRs. In the post-denitrifying MBBRs

(Torresi et al., 2017), additional carbon sources (i.e., methanol or ethanol) were spiked in the systems, which are known to be readily consumable substrates. This suggests that in the absence of catabolic limitation (i.e., in the presence of easily degradable organic carbon), biotransformation of the targeted pharmaceuticals may be more expedient under anoxic versus aerobic conditions.

(ii) An increase in biodiversity might not translate into differences in microbial functionality if the microbial community present sufficient biodiversity to begin with, that can saturate the possible effects (Johnson et al 2015a). While this effect was not observed for suspended biomass in full-scale WWTP (i.e., microbial communities were insufficiently biodiverse to maximize the collective rate of multiple micropollutant biotransformation, Johnson et al., (2015a)), this may be different for biofilm systems that can already potentially harbor higher microbial diversity compared to suspended biomass (Lu and Chandran, 2010; Stewart and Franklin, 2008).

Overall, our results (at both global and system level) suggest that despite the general positive association between microbial diversity and macro and microbial ecology activity (Cardinale et al., 2012; Emmett Duffy, 2009), this association is not fully understood for microbial communities in biological wastewater treatment regarding micropollutant biotransformation. On the other hand, additionally information could be obtained by targeting a broader number of micropollutants.

Nonetheless, few studies demonstrated the relationships between microbial diversity and system stability and resilience in wastewater treatment plant (Cook et al., 2006; Fernandez et al., 2000), which per se can be correlated with functional redundancy (Briones and Raskin, 2003). Accordingly, it has been suggested that if two denitrifying configurations perform equally efficiently, the configuration with higher functional diversity should be preferentially selected to ensure higher system stability (Lu et al., 2014).

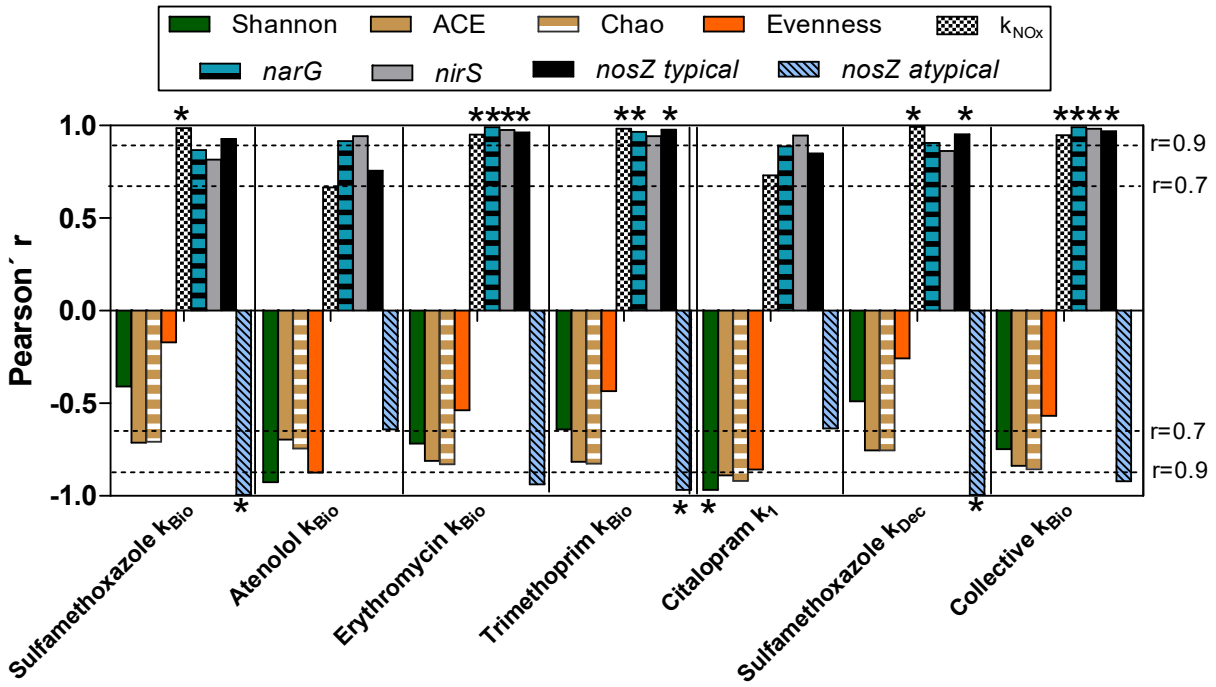

Figure 7. Pearson´s coefficient (r) of the correlation between biotransformation (k_{Bio}), retransformation (k_{Dec}) of micropollutant, collective k_{Bio} with Shannon biodiversity, richness (ACE and Chao), evenness indices (at 99% sequences similarity) and specific denitrification rate $\overline{k}_{NOX}$ (mgN g^{-1} d^{-1}) for Batch 2. Asterisks indicate significance ($p<0.05$).

4. Conclusions

Two pre-denitrifying MBBR systems were operated in parallel in single- (U) and three-stage (S) configurations using pre-clarified wastewater as influent and native concentration of micropollutants. The microbial communities in the two MBBR systems in terms of α- and β- diversity were investigated during long-term operation and compared to the performance.

- Staging of MBBR systems led to an increased richness of the microbial community at system level. Within the three-stage system, the decreasing gradient of organic carbon loading and availability was accompanied by an increase α-diversity of the microbial community.
- The microbial community became stable after 200 days operation, when the two configurations shared a core of OTUs such as *Burkholderiales*, *Xanthomonadales*, *Flavobacteriales* and *Sphingobacteriales.* The staged configuration (and in particular in the last stage MBBR, S3) selected for OTUs such as *Candidate division WS6* and *Deinococcales*.
- No major difference between S and U configurations was observed in terms of removal efficiency (%) or bio- and retransformation rate constants of sulfamethoxazole, atenolol, erythromycin, trimethoprim, citalopram, venlafaxine, ibuprofen, metoprolol and sulfamethizole.
- Specific and *collective* bio- and re-transformation rate constants of the targeted pharmaceuticals positively correlated with specific denitrification rates and abundance of denitrifying genes (*narG*, *nirS* and *nosZ* typical), rather than biodiversity.

Overall, staging of MBBR systems under denitrifying conditions resulted in enhanced denitrification rate and increased microbial diversity compared to a single-stage configuration, although no major improvement was observed in the removal of the selected trace organic pharmaceuticals.

Acknowledgments

This research was supported by MERMAID: an Initial Training Network funded by the People Programme (Marie-Curie Actions) of the European Union's Seventh Framework Programme FP7/2007-2013/under REA grant agreement n. 607492. The authors thank Luca Loreggian and Saverio Conti for technical support.

References

Altschul, S.F., Madden, T.L., Schäffer, A.A., Zhang, J., Zhang, Z., Miller, W., Lipman, D.J., 1997. Gapped BLAST and PSI-BLAST: a new generation of protein database search programs. Nucleic Acids Res. 25, 3389–402.

Arriaga, S., De Jonge, N., Lund Nielsen, M., Andersen, H.R., Borregaard, V., Jewel, K., Ternes, T.A., Lund Nielsen, J., 2016. Evaluation of a membrane bioreactor system as post-treatment in waste water treatment for better removal of micropollutants.

Barbosa, M.O., Moreira, N.F.F., Ribeiro, A.R., Pereira, M.F.R., Silva, A.M.T., 2016. Occurrence and removal of organic micropollutants: An overview of the watch list of EU Decision 2015/495. Water Res. 94, 257–279.

Birtel, J., Walser, J.-C., Pichon, S., Bürgmann, H., Matthews, B., 2015. Estimating Bacterial Diversity for Ecological Studies: Methods, Metrics, and Assumptions. PLoS One 10.

Braker, G., Zhou, J., Wu, L., Devol, A.H., Tiedje, J.M., 2000. Nitrite reductase genes (nirK and nirS) as functional markers to investigate diversity of denitrifying bacteria in pacific northwest marine sediment communities. Appl. Environ. Microbiol. 66, 2096–104.

Bray, J.R., Curtis, J.T., 1957. An Ordination of the Upland Forest Communities of Southern Wisconsin. Ecol. Monogr. 27, 325–349.

Briones, A., Raskin, L., 2003. Diversity and dynamics of microbial communities in engineered environments and their implications for process stability. Curr. Opin. Biotechnol. 14, 270–276.

Bryant, J.A., Stewart, F.J., Eppley, J.M., Delong, E.F., 2017. Microbial community phylogenetic and trait diversity declines with depth in a marine oxygen minimum zone. 93, 1659–1673.

Carballa, M., Omil, F., Lema, J.M., Llompart, M., García-Jares, C., Rodriguez, I., Gomez, M., Ternes, T., 2004. Behavior of pharmaceuticals, cosmetics and hor- mones in a sewage treatment plant. Water Res. 38 (12), 2918e2926.

Cardinale, B.J., Duffy, J.E., Gonzalez, A., Hooper, D.U., Perrings, C., Venail, P., Narwani, A., Mace, G.M., Tilman, D., A.Wardle, D., Kinzig, A.P., Daily, G.C., Loreau, M., Grace, J.B., Larigauderie, A., Srivastava, D.S., Naeem, S., 2012. Biodiversity loss and its impact on humanity. Nature 489, 326–326.

Chaturvedi, R., Archana, G., 2012. Novel 16S rRNA based PCR method targeting Deinococcus spp. and

its application to assess the diversity of deinococcal populations in environmental samples. J. Microbiol. Methods 90, 197–205.

Ciesielski, S., Kulikowska, D., Kaczowka, E., Kowal, P., 2010. Characterization of bacterial structures in a two-stage moving-bed biofilm reactor (MBBR) during nitrification of the landfill leachate. J. Microbiol. Biotechnol. 20, 1140–1151.

Criddle CS (1993) The kinetics of cometabolism. Biotechnol Bioeng 72: 1048–1056

Dickenson, E.R.V., Snyder, S.A., Sedlak, D.L., Drewes, J.E., 2011. Indicator compounds for assessment of wastewater effluent contributions to flow and water quality. Water Res. 45 (3), 1199e1212.

Dojka, M.A., Harris, J.K., Pace, N.R., 2000. Expanding the known diversity and environmental distribution of an uncultured phylogenetic division of bacteria. Appl. Environ. Microbiol. 66, 1617–21.

Dojka, M., Hugenholtz, P., Haack, S., Pace, N., 1998. Microbial diversity in a hydrocarbon-and chlorinated-solvent-contaminated aquifer undergoing intrinsic bioremediation. Appl. Environ. Microbiol. 64, 3869–3877.

Edgar, R.C., Haas, B.J., Clemente, J.C., Quince, C., Knight, R., 2011. UCHIME improves sensitivity and speed of chimera detection. Bioinformatics 27, 2194–200.

Falås, P., Wick, A., Castronovo, S., Habermacher, J., Ternes, T.A., Joss, A., 2016. Tracing the limits of organic micropollutant removal in biological wastewater treatment. Water Res. 95, 240–249.

Fischer, K., Majewsky, M., 2014. Cometabolic degradation of organic wastewater micropollutants by activated sludge and sludge-inherent microorganisms. Appl. Microbiol. Biotechnol. 98, 6583–97.

Hallin, S., Throbäck, I.N., Dicksved, J., Pell, M., 2006. Metabolic profiles and genetic diversity of denitrifying communities in activated sludge after addition of methanol or ethanol. Appl. Environ. Microbiol. 72, 5445–5452.

Helbling, D.E., Johnson, D.R., Lee, T.K., Scheidegger, A., Fenner, K., 2015b. A framework for establishing predictive relationships between specific bacterial 16S rRNA sequence abundances and biotransformation rates. Water Res. 70, 471–484.

Huston, M.A., 1994. Biological Diversity: the Coexistence of Species. Cambridge University Press.

Jobling, S., Nolan, M., Tyler, C.R., Geoff Brighty, A., Sumpter, J.P., 1998. Widespread Sexual Disruption in Wild Fish.

Johnson, D.R., Helbling, D.E., Lee, T.K., Park, J., Fenner, K., Kohler, H.P.E., Ackermann, M., 2015a.

254 Association of biodiversity with the rates of micropollutant biotransformations among full-scale
255 wastewater treatment plant communities. Appl. Environ. Microbiol. 81, 666–675.
256 Johnson, D.R., Lee, T.K., Park, J., Fenner, K., Helbling, D.E., 2015b. The functional and taxonomic
257 richness of wastewater treatment plant microbial communities are associated with each other and
258 with ambient nitrogen and carbon availability. Environ. Microbiol. 17, 4851–4860.
259 Johnson, D.R., Helbling, D.E., Men, Y., Fenner, K., 2015c. Can meta-omics help to establish causality
260 between contaminant biotransformations and genes or gene products? Environ. Sci. Water Res.
261 Technol. 1, 272–278.
262 Joss, A., Zabczynski, S., Göbel, A., Hoffmann, B., Löffler, D., McArdell, C.S., Ternes, T. a., Thomsen,
263 A., Siegrist, H., 2006. Biological degradation of pharmaceuticals in municipal wastewater
264 treatment: Proposing a classification scheme. Water Res. 40, 1686–1696.
265 Kampschreur, M.J., Temmink, H., Kleerebezem, R., Jetten, M.S.M., van Loosdrecht, M.C.M., 2009.
266 Nitrous oxide emission during wastewater treatment. Water Res. 43, 4093–4103.
267 Kolpin, D.W., Meyer, M.T., 2002. Pharmaceuticals , Hormones , and Other Organic Wastewater
268 Contaminants in U . S . Streams , 1999 - 2000 : A National Reconnaissance 36, 1202–1211.
269 Li, D., Alidina, M., Ouf, M., Sharp, J.O., Saikaly, P., Drewes, J.E., 2013. Microbial community evolution
270 during simulated managed aquifer recharge in response to different biodegradable dissolved organic
271 carbon (BDOC) concentrations. Water Res. 47, 2421–30.
272 Li, D., Sharp, J.O., Saikaly, P.E., Ali, S., Alidina, M., Alarawi, M.S., Keller, S., Hoppe-Jones, C.,
273 Drewes, J.E., 2012. Dissolved organic carbon influences microbial community composition and
274 diversity in managed aquifer recharge systems. Appl. Environ. Microbiol. 78, 6819–6828.
275 Lu, H., Chandran, K., 2010. Diagnosis and quantification of glycerol assimilating denitrifying bacteria
276 in an integrated fixed-film activated sludge reactor via 13C DNA stable-isotope probing. Environ.
277 Sci. Technol. 44 (23), 8943e8949.
278 Lu, H., Chandran, K., Stensel, D., 2014. Microbial ecology of denitrification in biological wastewater
279 treatment. Water Res. 64, 237–254. doi:10.1016/j.watres.2014.06.042
280 Margot, J.; Rossi, L.; Barry, D. A.; Holliger, C. A review of the fate of micropollutants in wastewater
281 treatment plants. Wiley Interdiscip. Rev.: Water 2015, 2 (5), 457−487
282 Marzorati, M., Wittebolle, L., Boon, N., Daffonchio, D., Verstraete, W., 2008. How to get more out of
283 molecular fingerprints: practical tools for microbial ecology. Environ. Microbiol. 10, 1571–81.

McMurdie, P.J., Holmes, S., 2013. phyloseq: an R package for reproducible interactive analysis and graphics of microbiome census data. PLoS One 8, e61217.

Naether, A., Foesel, B.U., Naegele, V., Wüst, P.K., Weinert, J., Bonkowski, M., Alt, F., Oelmann, Y., Polle, A., Lohaus, G., Gockel, S., Hemp, A., Kalko, E.K. V, Linsenmair, K.E., Pfeiffer, S.,

Renner, S., Schöning, I., Weisser, W.W., Wells, K., Fischer, M., Overmann, J., Friedrich, M.W., 2012. Environmental factors affect Acidobacterial communities below the subgroup level in grassland and forest soils. Appl. Environ. Microbiol. 78, 7398–406.

Ofiteru, I.D., Lunn, M., Curtis, T.P., Wells, G.F., Criddle, C.S., Francis, C.A., Sloan, W.T., 2010. Combined niche and neutral effects in a microbial wastewater treatment community. Proc. Natl. Acad. Sci. 107, 15345–15350.

Orellana, L.H., Rodriguez-R, L.M., Higgins, S., Chee-Sanford, J.C., Sanford, R.A., Ritalahti, K.M., Löffler, F.E., Konstantinidis, K.T., 2014. Detecting nitrous oxide reductase (NosZ) genes in soil metagenomes: method development and implications for the nitrogen cycle. MBio 5, e01193-14.

Painter, M.M., Buerkley, M.A., Julius, M.L., Vajda, A.M., Norris, D.O., Barber, L.B., Furlong, E.T., Schultz, M.M., Schoenfuss, H.L., 2009. Antidepressants at environmentally relevant concentrations affect predator avoidance behavior of larval fathead minnows (Pimephales Promelas). Environ. Toxicol. Chem. 28, 2677.

Pholchan, M.K., de Baptista, J.C., Davenport, R.J., Sloan, W.T., Curtis, T.P., 2013. Microbial community assembly, theory and rare functions. Front. Microbiol. 4, 1–9.

Plósz, B.G., 2007. Optimization of the activated sludge anoxic reactor configuration as a means to control nutrient removal kinetically. Water Res. 41, 1763–1773.

Plósz, B.G., Langford, K.H., Thomas, K. V, 2012. An activated sludge modeling framework for xenobiotic trace chemicals (ASM-X): assessment of diclofenac and carbamazepine. Biotechnol. Bioeng. 109, 2757–69.

Polesel, F., Torresi, E., Loreggian, L., Casas, M.E., Christensson, M., Bester, K., Plósz, B.G., 2017. Removal of pharmaceuticals in pre-denitrifying MBBR – Influence of organic substrate availability in single- and three-stage configurations. Water Res. 123, 408–419.

Price, M.N., Dehal, P.S., Arkin, A.P., 2009. FastTree: computing large minimum evolution trees with profiles instead of a distance matrix. Mol. Biol. Evol. 26, 1641–50.

Quast, C., Pruesse, E., Yilmaz, P., Gerken, J., Schweer, T., Yarza, P., Peplies, J., Glöckner, F.O., 2013.

314 The SILVA ribosomal RNA gene database project: improved data processing and web-based tools.
315 Nucleic Acids Res. 41, D590-6.
316 Rittmann, B.E., Smets, B.F., MacDonald, J. a, Stahl, D. a, 1995. Plasmid transfer for enhancing
317 degradation capabilities. Environ. Health Perspect. 103 Suppl, 113–5.
318 Roeleveld, P.J., Van Loosdrecht, M.C.M., 2002. Experience with guidelines for wastewater
319 characterisation in The Netherlands. Water Sci. Technol. 45, 77–87.
320 Sanford, R.A., Wagner, D.D., Wu, Q., Chee-Sanford, J.C., Thomas, S.H., Cruz-García, C., Rodríguez,
321 G., Massol-Deyá, A., Krishnani, K.K., Ritalahti, K.M., Nissen, S., Konstantinidis, K.T., Löffler,
322 F.E., 2012. Unexpected nondenitrifier nitrous oxide reductase gene diversity and abundance in soils.
323 Proc. Natl. Acad. Sci. U. S. A. 109, 19709–14.
324 Sathyamoorthy S, Chandran K, Ramsburg CA (2013) Biodegradation and cometabolic modeling of
325 selected beta blockers during ammo- nia oxidation. Environ Sci Technol 47:12835–12843
326 Schloss, P.D., 2009. Introducing mothur: A Computational Toolbox for Describing and Comparing
327 Microbial Communities. Abstr. Gen. Meet. Am. Soc. Microbiol. 109.
328 Scuras, S.E., Jobbagy, A., Leslie Grady, C.P., 2001. Optimization of activated sludge reactor
329 configuration:: kinetic considerations. Water Res. 35, 4277–4284. dSlade, D., Radman, M., 2011.
330 Oxidative Stress Resistance in Deinococcus radiodurans, Microbiology and Molecular Biology
331 Reviews.
332 Sözen, S., Çokgör, E.U., Orhon, D., Henze, M., 1998. Respirometric analysis of activated sludge
333 behaviour—II. Heterotrophic growth under aerobic and anoxic conditions. Water Res. 32, 476–488.
334 Stadler, L.B., Love, N.G., 2016. Impact of microbial physiology and microbial community structure on
335 pharmaceutical fate driven by dissolved oxygen concentration in nitrifying bioreactors. Water Res.
336 104, 189–199.
337 Stewart, P.S., Franklin, M.J., 2008. Physiological heterogeneity in biofilms. Nat Rev Micro 6, 199–210.
338 Suarez, S., Lema, J.M., Omil, F., 2010. Removal of Pharmaceutical and Personal Care Products (PPCPs
339) under nitrifying and denitrifying conditions. Water Res. 44, 3214–3224.
340 Tchobanoglous, G., Burton, F., Stensel, H., 2003.Wastewater Engineering: Treatment and Reuse, fourth
341 ed. Metcalf and Eddy, Inc., McGraw-Hill Company, New York
342 Ternes, T.A., 1998. Occurrence of drugs in German sewage treatment plants and rivers. Water Res. 32,
343 3245–3260.

Torresi, E., Casas, M.E.C., Polesel, F., Pl, B.G., Bester, K., 2017. Impact of external carbon dose on the removal of micropollutants using methanol and ethanol in post-denitrifying moving bed biofilm reactors 108, 95–105.

Torresi, E., Fowler, J.S., Polesel, F., Bester, K., Andersen, H.R., Smets, B.F., Plosz, B.G., Christensson, M., 2016a. Biofilm thickness influences biodiversity in nitrifying MBBRs – Implications on micropollutant removal. Environ. Sci. Technol. 50, 9279–9288.

Wells, G.F., Wu, C.H., Piceno, Y.M., Eggleston, B., Brodie, E.L., DeSantis, T.Z., Andersen, G.L., Hazen, T.C., Francis, C.A., Criddle, C.S., 2014. Microbial biogeography across a full-scale wastewater treatment plant transect: Evidence for immigration between coupled processes. Appl. Microbiol. Biotechnol. 98, 4723–4736.

Will, C., Thürmer, A., Wollherr, A., Nacke, H., Herold, N., Schrumpf, M., Gutknecht, J., Wubet, T., Buscot, F., Daniel, R., 2010. Horizon-specific bacterial community composition of German grassland soils, as revealed by pyrosequencing-based analysis of 16S rRNA genes. Appl. Environ. Microbiol. 76, 6751–9.

Yu, Y., Lee, C., Kim, J., Hwang, S., 2005. Group-specific primer and probe sets to detect methanogenic communities using quantitative real-time polymerase chain reaction. Biotechnol. Bioeng. 89, 670–9.

Zavaleta, E.S., Pasari, J.R., Hulvey, K.B., David Tilman, G., 2010. Sustaining multiple ecosystem functions in grassland communities requires higher biodiversity. Proc. Natl. Acad. Sci. 104, 1443–1446.

Zhang, Y., Ji, G., Wang, R., 2016. Drivers of nitrous oxide accumulation in denitrification biofilters with low carbon:nitrogen ratios. Water Res. 106, 79–85.

Ødegaard, H., 1999. The Moving Bed Biofilm Reactor. Water Environ. Eng. Reuse Water 250–305.